Shape coexistence and strongly coupled bands in ^{118}Sb

S. Y. Wang,[1,*] B. Qi,[1] D. P. Sun,[1] X. L. Ren,[1] B. T. Duan,[1] F. Chen,[1] C. Liu,[1] C. J. Xu,[1] L. Liu,[1] H. Hua,[2] Z. Y. Li,[2] J. M. Yao,[3] L. H. Zhu,[4] X. G. Wu,[4] G. S. Li,[4] Y. Liu,[4] X. Q. Li,[4] Y. Zheng,[4] L. L. Wang,[4] and L. Wang[4]

[1]*Shandong Provincial Key Laboratory of Optical Astronomy and Solar-Terrestrial Environment, School of Space Science and Physics, Shandong University at Weihai, Weihai 264209, People's Republic of China*

[2]*School of Physics, and SK Laboratory of Nuclear Physics and Technology, Peking University, Beijing 100871, People's Republic of China*

[3]*School of Physical Science and Technology, Southwest University, Chongqing 400715, People's Republic of China*

[4]*China Institute of Atomic Energy, Beijing 102413, People's Republic of China*

(Received 31 August 2010; published 24 November 2010)

Excited states of ^{118}Sb were populated via the ^{116}Cd(^{7}Li,5n)^{118}Sb fusion-evaporation reaction at a beam energy of 50 MeV. The previously known level scheme has been considerably extended, and about 36 new transitions were added into the level scheme of ^{118}Sb. One new rotational band has been identified, and assigned the $\pi g_{9/2}^{-1} \otimes \nu g_{7/2}$ configuration. The configuration-fixed constrained triaxial relativistic mean-field approaches and the particle-rotor model calculations are employed for analysis of the level structure of ^{118}Sb.

DOI: 10.1103/PhysRevC.82.057303 PACS number(s): 21.10.Re, 27.60.+j, 23.20.Lv, 21.60.Ev

The structure of excited states in nuclei near the $Z = 50$ magic number has recently provided a wealth of interesting physics. Nuclei near this closed proton shell exhibit a variety of collective structures that coexist with the single-particle structure. The coexistence of both collective and single-particle structures has been systematically observed in the Sn and Sb nuclei in the $Z \sim 50$ and $A \sim 110$ regions [1–5]. In general, single-particle structures are low in excitation energy. With increasing spin and excitation energy, collective structures were developed with moderate to large deformation through particle-hole excitations across the $Z = 50$ shell gap, from the β-upsloping $g_{9/2}$ orbital into the β-downsloping $g_{7/2}$ orbital. This presents the possibility of studying collective and noncollective effects within the same nuclear system. Another interesting area in this mass region is the phenomenon of shear bands. Such bands have been observed in even-even ^{106,108}Sn [6,7], odd-A ^{105}Sn [8], and odd-odd ^{108}Sb [9]. It is of particular interest to investigate the shear mechanism along an isotopic chain in this region. With a change in neutron number a gradual change in quadrupole deformation is explicit. This helps in understanding the relative contribution of core and shear mechanism in spin generation along a band for the same set of quasiparticles. In order to explore the systematic properties of these structure features to heavier nuclei, experiments have been performed to investigate ^{118}Sb.

Excited states of ^{118}Sb were populated in the ^{116}Cd(^{7}Li, 5n) fusion-evaporation reaction using a 50-MeV beam provided by the HI-13 tandem accelerator at the China Institute of Atomic Energy in Beijing. The ^{116}Cd target was a self-supporting foil of 2.5 mg/cm^2 in thickness. Twofold γ-γ coincident events were collected using an array of 12 Compton-suppressed HPGe detectors and two low-energy photon spectrometer (LEPS) detectors. Approximately 2×10^8 γ-γ coincidence events were collected during this experiment. The energy and intensity calibration of the Ge detectors were made by using the standard ^{152}Eu and ^{133}Ba radioactive sources. These data were gain matched and sorted into two matrices. The first matrix was created for all detectors against all detectors, used to deduce the level scheme of ^{118}Sb. The second matrix was constructed using the directional correlation of oriented (DCO) states method with one axis of the detectors lying at $\sim 45^\circ$ and the other at $\sim 90^\circ$ with respect to the beam direction. With setting gates on the stretched quadrupole transitions, DCO ratios were larger than 1.0 for stretched quadrupole transitions, and were less than 0.8 for pure dipole transitions in our array geometry. This empirical law can thus be used to assist us in the multipolarity assignments for newly observed rays. This data set had been utilized previously to establish the level scheme of ^{118}Sn [2].

The level scheme of ^{118}Sb obtained from the present work is shown in Fig. 1. A total of 36 new γ rays have been found and are indicated with asterisks in the level scheme in Fig. 1. The placement of the γ rays in the level scheme is based on their relative intensities, energy sums, and coincidence relationships. All γ rays reported in this work feed eventually toward an isomeric state at $I^\pi = 8^-$. For convenience, here this 8^- isomeric state is taken as zero of the energy scale. As shown in Fig. 1, the level scheme can be roughly separated into two independent parts. One part is irregular, exhibits the characteristics of the single-particle structures; the other part is systematic and band-like.

In the present work, about 15 new transitions are added into the left-hand side of Fig. 1, extending these single-particle levels to an excitation energy $\sim$4 MeV. These new transitions can be clearly seen in Fig. 2(a). The multipolarities for the observed transitions are based on those obtained from the previous work and measured DCO ratios. The 8^- isomeric state had been defined by magnetic moment measurements to be the $\pi d_{5/2} \otimes \nu h_{11/2}$ configuration [10]. The low-lying states with spin and parity $I^\pi = 7^-$ and 8^- may be interpreted as members of the $\pi d_{5/2} \otimes \nu h_{11/2}$ multiplet with an admixture of $\pi g_{7/2} \otimes \nu h_{11/2}$. The 10^- level at 1321 keV decaying into the 8^- isomer can be naturally described as a neutron 2^+ excitation coupled to the 8^- structure. The energy separation

*sywang@sdu.edu.cn

 ©2010 The American Physical Society

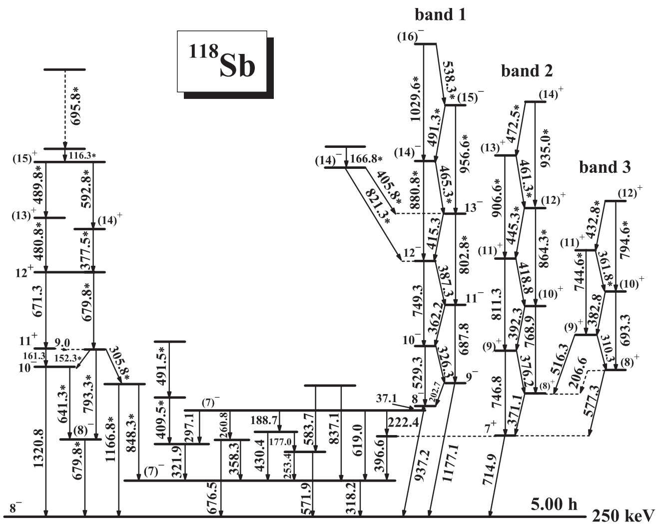

FIG. 1. Level scheme of ^{118}Sb proposed in the present work. New transitions observed in the present work are denoted with asterisks.

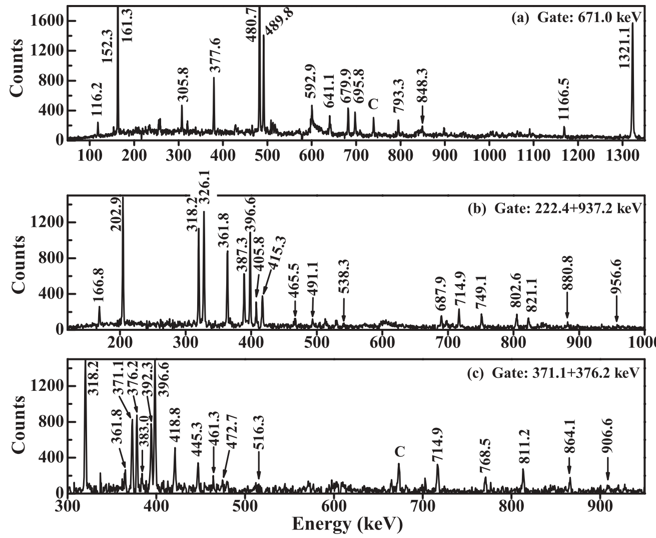

FIG. 2. Examples of γ-γ coincidence spectra in ^{118}Sb. (a) Inset shows the γ-ray spectrum gated on the 671.0 keV transition. (b) Inset displays transitions in band 1. (c) Inset displays transitions in band 2. The peaks labeled C indicate contaminations.

of 1321 keV between the 10^- state and the 8^- isomer is almost equal to the energy of the 2_1^+ level in the ^{116}Sn [11]. Above the 1321 keV level the negative parity is changed to positive parity by the 161.3 keV $E1$ transition indicating spin and parity $I^\pi = 11^+$ for the state at 1482 keV. The level energy spacing between the 11^+ state and the 8^- isomer is also similar to those between the $11/2^-$ state and the $5/2^+$ ground state in ^{117}Sb [12], and therefore, we associate the 11^+ state with the $\pi h_{11/2} \otimes \nu h_{11/2}$ configuration. The level at 2153 keV has been assigned $I^\pi = 12^+$ [13]. This assignment is further supported by the present measured DCO ratios of 671.3 keV transitions. Based on the measured DCO ratios, we have assigned an $E2$ multipolarity for the 377.5 and 489.8 keV γ rays, and a $M1/E2$ for the 480.8 keV transition. Thus, new 2531, 2634, and 3124 keV levels are suggested as the spin parity of $(14)^+$, $(13)^+$, and $(15)^+$, respectively. Owing to the poor statistics, the DCO ratios for the 116.3 and 695.8 keV transitions cannot be obtained accurately.

On the right-hand side of Fig. 1, three strongly coupled bands are constructed and labeled 1, 2, and 3. Two examples of γ-ray spectra of the rotational bands are presented in Figs. 2(b) and 2(c). Band 1 is the most strongly populated of the rotational bands, and has been already assigned to the $\pi g_{9/2}^{-1} \otimes \nu h_{11/2}$ configuration [14]. Band 1 has been extended from $I = 13^-$ to $(16)^-$ in the present work. The second band (band 2) was built on the 22 ns 7^+ isomeric state [15]. This band had been previously observed from the $I^\pi = 7^-$ band head to the $I^\pi = 11^-$ state, but has been extended up to $I^\pi = (14)^-$ in this work. On the basis of magnetic moment measurements [16], band 2 was proposed to be built predominantly on the $\pi g_{9/2}^{-1} \otimes \nu d_{5/2}$ configuration. Prior to this work, only two transitions belonging to band 3 were reported by Fayez-Hassan *et al.* [15], but no interpretation was made at that time. In the present work, two-dipole and three-quadrupole transitions are identified, which then established a new coupled band structure (labeled 3). Similar to band 2, band 3 is also strongly coupled in nature. Three linking transitions between bands 2 and 3 have been already reported in Refs. [13,15]. Furthermore, the levels with the same spin and parity in both bands 2 and 3 lie very close in energy, as one would expect for a chiral doublet band, which had already been reported in the $A \sim 100$ and 130 mass regions. However, the chiral speculation can be ruled out because the calculated shape turns out to be axial for band 2. Here, we suggest that they belong to pseudospin doublet bands. This can be supported by the following particle-rotor model (PRM) calculations.

The configuration-fixed constrained triaxial relativistic mean-field (RMF) approaches were first applied to determine the quadrupole deformations for the different configurations. A detailed description of this approach with nucleon-nucleon interactions can be found in Ref. [17], and references therein. Self-consistent deformation parameters $\beta_2 \sim 0.17$ and $\gamma \sim 60^\circ$ are obtained from the present RMF approaches corresponding to the $\pi d_{5/2}(g_{7/2}) \otimes \nu h_{11/2}$ configuration. In contrast, configurations involving the $g_{9/2}[404]\frac{9}{2}$ proton (e.g., $\pi g_{9/2}^{-1} \otimes \nu h_{11/2}$, $\pi g_{9/2}^{-1} \otimes \nu d_{5/2}$, and $\pi g_{9/2}^{-1} \otimes \nu g_{7/2}$) are predicted to possess the prolate quadrupole deformations, $\beta_2 \sim 0.23$ and $\gamma \sim 0^\circ$. Based on the present RMF approaches, the 8^- isomeric state based on the $\pi d_{5/2} \otimes \nu h_{11/2}$ configuration has an oblate shape. A number of single-particle levels decaying into this isomer indicate that the 8^- isomer is the noncollective oblate deformation $\gamma = +60^\circ$. Therefore, the coexisting collective and the single-particle structures in ^{118}Sb should be contributed to the shape coexistence of the noncollective oblate shape ($\gamma = +60^\circ$) and collective prolate shape ($\gamma = 0^\circ$). Furthermore, the RMF approaches also predict a superdeformed state ($\beta_2 \sim 0.41$, $\gamma \sim 15^\circ$), corresponding to the $\pi h_{11/2} \otimes \nu h_{11/2}$ configuration.

To obtain further insight into the rotational bands of ^{118}Sb, we performed the PRM calculations with configurations of a $g_{9/2}$ proton hole and a quasineutron. Based on the above RMF approaches, the same deformation parameters $\beta_2 = 0.23$ and $\gamma = 0^\circ$ are used for bands 1, 2, and 3. To calculate

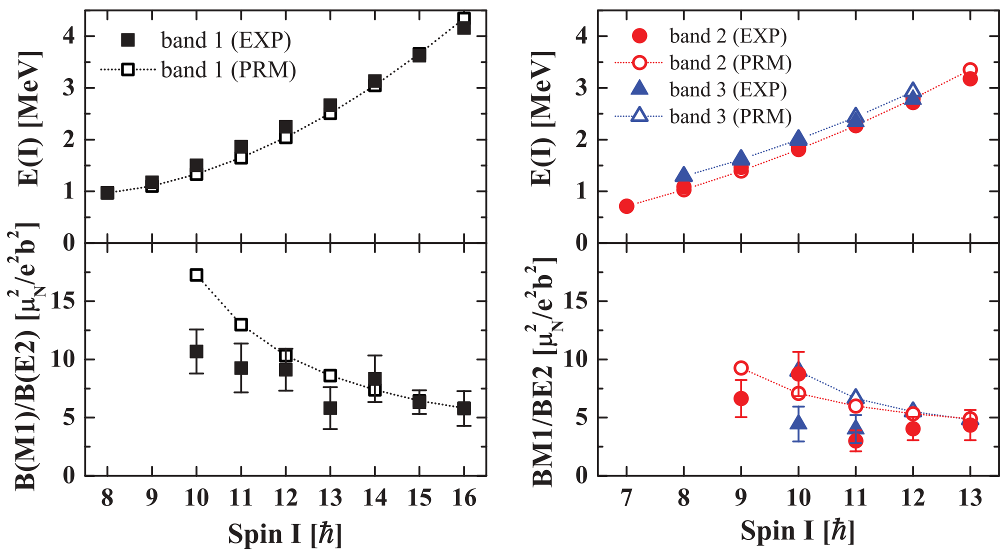

FIG. 3. (Color online) Plot of the excitation energies $E(I)$ and the $B(M1)/B(E2)$ ratios for bands 1, 2, and 3 as a function of spin. The filled (open) symbols are for the experimental (calculated) values. The calculated values are shifted in order to coincide with the experimental energy at the band head.

the electromagnetic transitions, we used a collective g factor for the core of $g_R = Z/A$ and an effective value of the free nucleon factor $g_s^{\rm eff} = 0.6 g_s^{\rm free}$. The quadrupole moment was calculated according to the liquid drop formula to be $3eb$. The other parameters used in the calculations are listed in Table I. More information on such calculations can be found in Refs. [18–20].

The experimental energy spectra $E(I)$ and $B(M1)/B(E2)$ ratios for coupled bands 1−3 are shown in Fig. 3, along with predictions from the PRM model for the proposed $\pi g_{9/2}^{-1} \otimes \nu h_{11/2}$, $\pi g_{9/2}^{-1} \otimes \nu d_{5/2}$, and $\pi g_{9/2}^{-1} \otimes \nu g_{7/2}$ configurations for comparison. The experimental $B(M1)/B(E2)$ ratios were deduced from the γ intensities by using relation (1) of Ref. [21]. The agreement between experiment and theory is good for bands 1–3, thereby supporting the configuration assignments proposed for these bands. Based on the present configuration assignments, bands 2 and 3 should be a pair of pseudospin partner bands. The energy difference between the band heads of band 2 ($I = 7\hbar$) and band 3 ($I = 8\hbar$) is 577 keV, which is close to the energy difference between the Nilsson states $g_{7/2}[402]5/2^+$ and $d_{5/2}[422]3/2^+$ in this mass region.

As mentioned in above, another interesting feature of this mass region is the magnetic rotational band. Such bands have been observed in even-even ^{106,108}Sn [6,7], odd-A ^{105}Sn [8], and odd-odd ^{108}Sb [9]. In the odd-odd Sb isotopes, the yrast band of ^{108}Sb ($N = 57$) has been interpreted as the magnetic rotational band in terms of the tilted axis cranking (TAC) model [9]. Calculations carried out using the TAC model [9] indicate a quadrupole deformation of $\epsilon_2 = 0.11$ for this structure. The interpretation of the magnetic rotational band means that the component of collective rotation of the core is small relative to the shear component. However, as deformation increases, competition is expected between these two modes of angular momentum generation. In order to better understand this competition, it is important to investigate the shear mechanism along an isotopic chain ranging from nearly spherical shapes, cases of pure shears, to significant deformations, where collective rotation dominates. The present RMF calculations predict the yrast band of ^{118}Sb was a $\beta_2 = 0.23$ prolate deformation. In order to show the picture more clearly and examine the evolution of two modes of angular momentum generation, we calculated for the yrast band of ^{118}Sb the expectation values of the squared angular momentum components for the total nucleus, the valence neutron, and proton at spin $I = 8$, 12, and 16 using the resulting wave functions of the PRM calculations (Fig 4). Figure 4 shows that the orientations of the valence proton and neutron are almost invariable, and the total angular momentum gradually aligns along the rotational axis (one axis) from $I = 8$ to 16. This is the typical case of collective (electric) rotational bands. In the odd-odd Sb isotopes, the yrast bands of ^{110}Sb($N = 59$) and ^{112}Sb($N = 61$) are predicted to exhibit the shear mechanism [22]. However, the recent lifetime measurements [23] for ^{112}Sb indicate that the $B(M1)$ shows

TABLE I. The parameters adopted for ^{118}Sb in the present PRM calculations.

Band	Configuration	$\mathcal{J}$ ($\hbar^2$/MeV)	Δ_n (MeV)	λ_n (MeV)	g_p	g_n
1	$\pi g_{9/2}^{-1} \otimes \nu h_{11/2}$	17	1.0	−1.605	1.261	−0.209
2	$\pi g_{9/2}^{-1} \otimes \nu d_{5/2}$	22	1.0	−0.378	1.261	−0.459
3	$\pi g_{9/2}^{-1} \otimes \nu g_{7/2}$	22	1.0	0.316	1.261	0.255

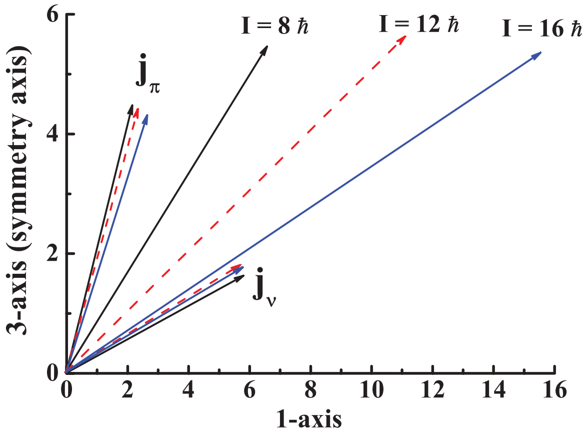

FIG. 4. (Color online) The angular momentum composition of the proton j_π and neutron j_ν, and total angular momentum I in PRM for band 1 are illustrated at spins $I = 8\hbar$, $12\hbar$, and $16\hbar$.

a small decrease with increasing spin. The $B(E2)$ values are considerably higher than those observed in the neighboring nuclei, which are known to exhibit the shear mechanism. This indicates the rotation of the core is the dominant contribution to the generation of angular momentum. Thus, ^{110}Sb($N = 59$) should be expected to exhibit the competition between the shear mechanism and collective rotation. The precise lifetime measurements for this band in ^{110}Sb are highly desirable in addressing the interesting question of the competition between the shear mechanism and collective rotation.

In summary, excited states of ^{118}Sb were populated via the ^{116}Cd(^{7}Li,5n)^{118}Sb reaction at a beam energy of 50 MeV. The previously known level scheme has been considerably extended, and about 36 new transitions were added into the level scheme of ^{118}Sb. One new rotational band has been identified, and assigned the $\pi g_{9/2}^{-1} \otimes \nu g_{7/2}$ configuration. The configuration-fixed constrained triaxial RMF approaches and the PRM calculations were employed for analysis of the level structure of ^{118}Sb.

This study is supported by the National Natural Science Foundation (Grant Nos. 10875074 and 11005069), the Independent Innovation Foundation of Shandong University (IIFSDU), and the Major State Research Development Programme (No. 2007CB815005) of China.

[1] J. Bron *et al.*, Nucl. Phys. A **318**, 335 (1979).
[2] S. Y. Wang *et al.*, Phys. Rev. C **81**, 017301 (2010).
[3] R. Duffait, J. van Maldeghem, A. Charvet, J. Sau, K. Heyde, A. Emsallem, M. Meyer, R. Beraud, J. Treherne, and J. Genevey, Z. Phys. A **307**, 259 (1982).
[4] G. J. Lane *et al.*, Phys. Rev. C **55**, R2127 (1997).
[5] G. J. Lane *et al.*, Phys. Rev. C **58**, 127 (1998).
[6] D. G. Jenkins *et al.*, Phys. Lett. B **428**, 23 (1998).
[7] D. G. Jenkins *et al.*, Phys. Rev. Lett. **83**, 500 (1999).
[8] A. Gadea *et al.*, Phys. Rev. C **55**, R1 (1997).
[9] D. G. Jenkins *et al.*, Phys. Rev. C **58**, 2703 (1998).
[10] P. T. Callaghan, M. Shott, and N. J. Stone, Nucl. Phys. A **221**, 1 (1974).
[11] A. Savelius *et al.*, Nucl. Phys. A **637**, 491 (1998).
[12] D. R. LaFosse, D. B. Fossan, J. R. Hughes, Y. Liang, H. Schnare, P. Vaska, M. P. Waring, and J.-y. Zhang, Phys. Rev. C **56**, 760 (1997).
[13] K. Kitao, Nucl. Data Sheets **75**, 99 (1995).
[14] S. Vajda *et al.*, Phys. Rev. C **27**, 2995 (1983).
[15] M. Fayez-Hassan *et al.*, Nucl. Phys. A **624**, 401 (1997).
[16] M. Ionescu-Bujor, A. Iordanescu, G. Pascovici, and V. Sabaiduc, Phys. Lett. B **200**, 259 (1988).
[17] J. Meng, J. Peng, S. Q. Zhang, and S. G. Zhou, Phys. Rev. C **73**, 037303 (2006).
[18] S. Q. Zhang, B. Qi, S. Y. Wang, and J. Meng, Phys. Rev. C **75**, 044307 (2007).
[19] S. Y. Wang, S. Q. Zhang, B. Qi, and J. Meng, Phys. Rev. C **75**, 024309 (2007).
[20] S. Y. Wang, S. Q. Zhang, B. Qi, J. Peng, J. M. Yao, and J. Meng, Phys. Rev. C **77**, 034314 (2008).
[21] S. Y. Wang *et al.*, J. Phys. G **32**, 283 (2006).
[22] Amita, A. K. Jain, and B. Singh, At. Data Nucl. Data Tables **74**, 283 (2000).
[23] A. Y. Deo, S. K. Tandel, S. B. Patel, P. V. Madhusudhana Rao, S. Muralithar, R. P. Singh, R. Kumar, R. K. Bhowmik, and Amita, Phys. Rev. C **71**, 017303 (2005).